DOE/BC/14896--9

--9

GEOLOGICAL AND PETROPHYSICAL CHARACTERIZATION OF THE FERRON SANDSTONE FOR 3-D SIMULATION OF A FLUVIAL-DELTAIC RESERVOIR

(Contract No. DE-AC22-93BC14896)

Utah Geological Survey (UGS), Salt Lake City, Utah 84109

Submitted: October 30, 1995

Contract Date: September 29, 1993

Anticipated Completion Date: September 29, 1996

Government Award (fiscal year): $ 1,225,482

Principal Investigator: M. Lee Allison, UGS

Program Manager: Thomas C. Chidsey, Jr., UGS

Contracting Officer's Representative: Robert Lemmon, Bartlesville Project Office

Reporting Period: July 1 - September 30, 1995

Objective

The objective of this project is to develop a comprehensive, interdisciplinary, and quantitative characterization of a fluvial-deltaic reservoir which will allow realistic inter-well and reservoir-scale modeling to be constructed for improved oil-field development in similar reservoirs world-wide. The geological and petrophysical properties of the Cretaceous Ferron Sandstone in east-central Utah will be quantitatively determined. Both new and existing data will be integrated into a three-dimensional representation of spatial variations in porosity, storativity, and tensorial rock permeability at a scale appropriate for inter-well to regional-scale reservoir simulation. Results could improve reservoir management through proper infill and extension drilling strategies, reduction of economic risks, increased recovery from existing oil fields, and more reliable reserve calculations. Transfer of the project results to the petroleum industry is an integral component of the project.

Summary of Technical Progress

Technical progress this quarter is divided into regional stratigraphy, case studies, stochastic modeling and fluid-flow simulation, and technology transfer activities. The regional stratigraphy of the Ferron Sandstone outcrop belt from Last Chance Creek to Ferron Creek is being described and interpreted (Fig. 1). Photomosaics and a database of existing surface and subsurface data are being used to determine the extent and depositional environment of each parasequence, and the nature of the contacts with adjacent rocks or flow units.

Detailed geological and petrophysical characterization of the primary reservoir lithofacies typically found in a fluvial-dominated deltaic reservoir, is continuing at selected case-study areas. Interpretations of lithofacies, bounding surfaces, and other geologic information are being combined with permeability measurements from closely spaced traverses and from drill-hole cores (existing and two drilled during the quarter). Petrophysical and statistical analyses are being incorporated with the geological characterization to develop a three-dimensional model of the reservoirs through fluid-flow simulation. Technology transfer consisted of seven presentations of project results to professional geologists and two project overviews presented to the news media, county and other government officials, and local industry representatives.

Regional Stratigraphy

The Utah Geological Survey (UGS) continues to combine digitized land-based and aerial photographs of the Ferron Sandstone outcrop belt into reproducible photomosaics using image-editing software. A total of 1823 photos depict 80 miles of Ferron Sandstone outcrop. Interpretations of parasequence boundaries, lithofacies, and various field data (such as measured section and gamma-ray transect locations) are being plotted on the photomosaics as part of both the regional and case-study analyses. These interpretations are being checked in the field at the same time the photomosaics are given vertical and horizontal scales.

During the quarter considerable effort was devoted to dividing the Ferron Sandstone into parasequences and parasequence sets (Fig. 2). Van Wagoner *et al.*[1] defined a parasequence as "a relatively conformable succession of genetically related beds or bedsets bounded by marine-flooding surfaces or their correlative surfaces." This definition is clear and precise. It is easy, using this definition, to draw diagrammatic cross sections distinguishing parasequences and the parasequence sets (grouping of parasequences that display a recognizable pattern of organization). In the Ferron Sandstone, distinguishing exactly what is and what is not a parasequence can be quite easy or extremely difficult. Parasequences, for the Ferron project, equate to shoreline sandstone bodies. In order to qualify as a parasequence, a unit must be bounded by surfaces that can be demonstrated as transgressive surfaces, or that at least manifest most of the key characteristics of transgressive surfaces. Bedding surfaces are being used to divide a shoreline sandstone body that defines a parasequence into units that represent distinct depositional episodes. Perhaps a quarter to a half of the parasequences recognized in the Ferron can be divided into smaller-scale units, and these will be incorporated into the stratigraphic scheme as it develops. Parasequences may be divided into smaller-scale genetic units, usually represented by upward-coarsening successions. However, in practice many sequence stratigraphers place parasequence boundaries at the top and bottom of each and every upward-coarsening succession that can be distinguished. The assumptions are that

if an upward-coarsening succession of shallow-marine strata is overlain by another such succession, deepening of water occurred at the boundary between the two. Deepening of water is the result of rising of sea level, and rising of sea level results in transgression. Therefore, such a boundary is a marine-flooding surface. This line of reasoning is often right, but not always. There are other processes that can lead to stacking of upward-coarsening successions. Wave-energy levels incident on a coastline could change as a function of climatic change. Sediment supply and the ratio of coarse to fine material could change as a function of a number of processes. Most importantly, along deltaic coasts, progradation and abandonment of delta lobes can cause changes both in sediment supply and wave energy.

Figure 2 shows all of the Ferron parasequences that have been recognized by the project team, named, and placed in their relative positions. The abundance of parasequences in parasequence sets Kf-1 and Kf-2, as compared to the younger parasequence sets, is striking. This is the result of two factors. First, Kf-1 and Kf-2 prograded farther into the basin than did later parasequence sets and so would be expected to be made up of more "building blocks." To draw a crude analogy; a longer tier of bricks has more bricks in it than does a short tier. The second factor hinges on the fact that the amount of relative sea-level rise that occurred during progradation was greater for the younger Ferron parasequence sets than it was for the older ones. This affected parasequence-level stratigraphy profoundly and requires some explanation. During progradation of parasequence sets Kf-1 and Kf-2, the supply of sediment was abundant compared to the creation of space in the basin to accommodate it. A relatively small amount of sediment was required to aggrade the coastal plain and a considerable proportion passed through the fluvial systems to reach the shoreline. Rapid supply of sediment at the river mouths promoted the building of river-dominated deltas, the deposits of which are conspicuously more abundant in Kf-1 and Kf-2 than they are in Kf-4 through Kf-7. It is highly probably that rises of relative sea level caused either by eustatic fluctuations or by pulses of basin subsidence continually affected the area and are the underlying mechanism for inducing parasequence-level transgressions and regressions. A delta is very much "at risk" should even a minor rise of relative sea level occur. Transgression of the coasts adjacent to a delta diminishes the rivers already inefficient gradient, leading inevitably to avulsion of the river, abandonment of the delta, and rapid transgression across the delta plain. Many such transgressions are recognizable in Kf-1 and Kf-2.

In the case of parasequence sets Kf-4 through Kf-7 (Kf-3 being something of an in-between case), the volume of sediment delivered to the area was much less compared to the rate of creation of accommodation space. And the rate decreased through time, resulting in overall backstepping of the parasequence sets. As a consequence, an increasingly large volume of sediment was required to aggrade the coastal plain behind the shoreline; less and less came through the fluvial systems to nourish the shoreline. The lower sediment supply tipped the balance in favor of the process of wave reworking. Major delta lobes did not form, the sediment being more evenly distributed along the coast. Minor rises of relative sea level had little effect on the shoreline. Transgressions probably did occur, but over limited distances.

The earliest, proximal part of each parasequence consists of deposits from wave-modified coasts. The relative sea level rises that brought about the parasequence-level transgressions caused reduction of sediment supply to the coasts. As the rise slowed and the balance shifted back to progradation, the supply of sediment to the coast increased. Initially, the supply was low, allowing extensive wave reworking. This also explains the pronounced seaward stratigraphic rise of many parasequences just seaward of their pinch-outs. The more distal parts of parasequences commonly

contain deltaic deposits. At these times, the rates of rise of relative sea level were slower and the amounts of sediment delivered to the shorelines were correspondingly greater. The supply was great enough to allow progradation of recognizable deltas, particularly in the cases of parasequence sets Kf-1 and Kf-2.

Case Studies

Core-Hole Program

Two stratigraphic test wells were drilled in the Ivie Creek case-study site: the Ivie Creek Nos. 10 and 11. These wells were designed to evaluate the lithofacies and reservoir characteristics of the Kf-1 and Kf-2 parasequence sets. The total depths of the wells are 420 and 444 ft respectively. These wells were located far enough back from the outcrop to avoid the coal burn zones encountered during the 1994 drilling program. Core and geophysical logs from these wells will provide data for a three-dimensional morphologic interpretation of individual lithofacies and capture the various reservoir changes in the Kf-1 and Kf-2 parasequence sets over an area analogous in size to a small oil field. The Kf-1 represents a river-dominated delta deposit which changes from proximal to distal (where the sandstone pinches out) from east to west across the Ivie Creek area. The Kf-2 contains more and cleaner sand, indicating a more wave-modified environment of deposition.

A total of 156 ft of core was recovered from the Ivie Creek No. 11 well. This core is stored at the UGS Sample Library and is available for study. The Ivie Creek No. 10 was not cored. Geophysical logs run in the Ivie Creek Nos. 10 and 11 wells include the formation density, caliper, and gamma ray. Sonic, dipmeter, and dual-spaced neutron logs were recorded in the Ivie Creek No. 11 well; these logs could not be run in the Ivie Creek No. 10 well since it would not hold water due to a large fracture zone.

Field Work

Several outcrop sections through the Kf-1 and Kf-2 parasequence sets were described in the Ivie Creek and Willow Creek Wash case-study areas (Fig.1). Description of the individual units in the outcrop sections include the following information: (1) primary and secondary lithology, composition, color, and grain size of the rocks; (2) sedimentary structures, biologic structures, and fossils in the rocks; and (3) bounding surfaces and depositional environment of the unit. These sections are being correlated with the 50 sections measured during the 1994 field season to develop interpretations of the stratigraphy and lithofacies. Paleocurrent measurements have also been made at Ivie Creek and in the Willow Creek Wash case-study areas. Photomosaics in both areas were scaled and interpretations completed.

Gamma-Ray Measurements

Outcrop gamma-ray measurements were completed along 14 permeability and petrophysical transects to: (1) determine variations in clay-mineral content (or sandstone/shale ratios), (2) permit detailed correlation among outcrop traverses and between the traverses and core-hole gamma-ray logs, and (3) detect possible diagenetic changes associated with precipitation of uranium. Field measurements were taken using a portable 256-channel gamma-ray spectrometer capable of

determining total natural gamma counts as well as concentrations of potassium, thorium, and uranium. Each transect consisted of 200 to 400 measurements at 0.5- to 1.0-ft intervals. Gamma-ray spectrometer readings are related to clay content in shaly sandstones; clay content influences the compartmentalization of flow units.

Core-Plug Sampling

The objective of core-plug sampling in the Ivie Creek case-study area was to characterize vertical and lateral variations of a number of petrophysical properties (velocity, density, porosity, permeability, and mineralogy) and to determine the interrelations among these properties in the Kf-1 and Kf-2 parasequence sets. The technique involved drilling 1- to 4-in.-long core plugs, 1 in. in diameter, with a portable gas-powered drill and diamond bit. The geographic orientation of each sample was determined and the sedimentary structures of the bed photographed. All core-plugging was done along vertical or near-vertical (depending on access) traverses with one sample per "bed" and about 30 to 50 samples per transect.

One significant change from the 1994 sampling program was a greatly increased emphasis on sampling for anisotropy studies: rather than taking just one horizontal sample per site, a set of three samples (horizontal, vertical, and 45°) was taken. Anisotropy is a variable that needs to be considered in the fluid-flow modeling. It is also a much broader petrophysical concern because anisotropy can be caused by either mineral alignment (platy, subhorizontal clay minerals) or by microfractures (usually one set of vertical microfractures); both causes affect fluid flow.

A total of 208 horizontal samples were taken from 10 traverses and 77 three-dimensional sets from eight traverses. These traverses correspond to permeability transects, measured sections, and gamma-ray transects.

Mini-Permeameter Measurements

A large quantity of new permeability data was collected during the quarter from both the Kf-1 and Kf-2 parasequence sets along 15 permeability transects (in addition to the seven transects from the 1994 field season) in the Ivie Creek case-study area (Fig. 3). Transect locations contained examples of the majority of the lithofacies present in the delta-front sequences. An electronic, miniprobe permeameter (mini-permeameter) supplied by the Mobil Exploration/Producing Technical Center was used to make laboratory permeability measurements on trimmed, whole core plugs taken from the outcrops. Measured stratigraphic sections were tied to the permeability transects.

A total of 1954 tests were performed on 1622 core plugs taken along the transects. Each sample was washed then dried in an oven for two days in an effort to ensure that all moisture was removed from the samples prior to testing. Core plug locations in 1995 were selected to accomplish several goals: (1) better characterize permeability distributions within clinoforms found within the Kf-1a parasequence, (2) evaluate both north-south and east-west variations in permeability structure within the Kf-2 parasequence set, and (3) evaluate two-dimensional and three-dimensional permeability anisotropy within different units of the Kf-2.

The lab permeability results, when combined with field and lab measurements taken during the 1994 field season and detailed geologic mapping, will be used to determine the statistical structure of the spatially variable permeability field within the delta front and to investigate how geological processes control the spatial distribution of permeability.

Clinoform Features of the Kf-1a Parasequence. Core plugs were collected along six short vertical transects (T9, T10, T11, T12, T14, and T15) and one horizontal transect (T16) in the vicinity of the 1994 transects T3 and T4 (circled area in Fig. 3). These plugs were obtained to characterize typical clinoform features found within the Kf-1a parasequence at the Ivie Creek case-study area. Core plugs were collected at 0.3-ft spacing along vertical transects and at 3.0-ft spacing along the horizontal transect. In addition, a series of vertical and horizontal core plug pairs were collected near transects T9, T10, T12, and T14 to develop a better understanding of permeability anisotropy in the vertical plane associated with specific sedimentary structures found within the clinoforms.

The site of transect T9 was chosen to sample much higher permeability rocks within the Kf-1a than were found in the 1994 season. Permeability values for several core plugs exceeded 300 millidarcies (md). More than 50% of the cores yielded permeability values in the 10 to 40 md range. Although permeability results obtained for transects T12, T14, T15, and T16 did not generally exceed 100 md, more than 50% of the cores yielded permeability values in the 10 to 40 md range. These results suggest that higher-permeability regions are present at more proximal positions within the clinoform structures of the Kf-1a. Transects T10 and T11 yielded lower-permeability results that confirm the expectation that more distal positions within the clinoform structures contain relatively low permeability rocks.

Vertical Variations and Anisotropy in the Vertical Plane within the Kf-2. Core plugs were collected from several locations in the Kf-2 to obtain insight into the two-dimensional and three-dimensional permeability anisotropy associated with specific sedimentary structures. The DC series of core plugs (Fig. 3) were collected to study the influence of cross bedding and soft-sediment deformation structures on anisotropy. Preliminary interpretation suggests that permeability anisotropy is less than one order of magnitude and may range from 2 to 5.

Figure 4 illustrates preliminary permeability profiles for transects T8, T20, and T19. First, it is important to note that much higher permeabilities are found in the more wave-modified facies of the Kf-2 when compared to the fluvial-dominated facies of the Kf-1. Second, even in the absence of correlations with geological data it is clear that strong vertical variations in permeability are indicated within the Kf-2. It is expected that many distinct permeability transitions will correspond to specific stratigraphic boundaries.

Petrophysical Analysis

Petrophysical measurements were made on 182 Ferron core plugs collected during the 1994 field season processed through Amoco Production Research's Geoscience Evaluation Module (GEM). The measurements consisted of: (1) saturated, dry, and grain densities (Fig 5a), (2) effective and Boyle's Law porosities (Fig. 5b), (3) air permeability (Fig. 5c), (4) magnetic susceptibility, (5) qualitative and quantitative mineralogy, (6) compressional and shear wave velocities as a function of effective pressure, and (7) thin-section-image analysis. The specific details of the GEM procedures used are given by Sondergeld and Rai.[2-4] Velocities were measured using the pulse transmission technique of Schreiber, et al.[5] and mineralogy was determined using a transmission infrared technique described by Griffiths and de Haseth.[6]

The major findings from preliminary analyses of these data are: (1) microfractures affect the velocity of all samples; however, microfractures have little significant influence on permeabilities, except perhaps for the least permeable samples; (2) permeability is very closely related to porosity,

with a linear relationship between porosity and the logarithm of permeability (Fig. 6a) that is roughly similar to those found from other high-porosity sedimentary rocks. That relationship, however, varies so much between formations in different parts of the world that it must be locally determined. The relationship for the Ferron Sandstone is much better than was anticipated based on porosity/mini-permeameter measurements made at the University of Utah (Fig 6b), and it extends to permeabilities far below the 2-md threshold for useful mini-permeameter measurements. This relationship means that permeability can be estimated for all core-plug samples for which measured porosity has been obtained. In addition, permeability logs can be estimated from density well logging; and (3) the dominant mineralogic control on velocity, porosity, and therefore permeability appears to be calcite cementation, not clay content, at least for the low-clay samples that have been measured to date. Quartz cementation probably also affects these parameters, but the Amoco measurements cannot distinguish quartz grains from quartz cement. Clay content certainly does decrease porosity and permeability, but this influence is not as linear as had been anticipated. For example, comparisons of outcrop gamma-ray measurements with mini-permeability results, as well as comparisons of Amoco determined mineralogy to Amoco determined permeability, show only a rough, qualitative correspondence. Consequently, one cannot expect to use the gamma-ray traverses to quantitatively estimate permeability, though they can indicate locations of minimal-permeability shales and fluid-flow bounding units.

Thin section were made from selected core plugs having varied lithology, clinoform position, and permeability values in the Kf-1a parasequence. The samples are quartz-rich sandstones with a complex diagenetic history. The sandstones show considerable compaction and little remaining primary porosity. Where porosity is present, it is largely secondary porosity developed from the dissolution of carbonate and dolomite cement. Early cements appear to be calcite, dolomite, and kaolinite. Iron (hematite) cement appears to be the last diagenetic cement. As expected medium- to coarse-grained sandstones have better porosity than fine-grained sandstones to siltstones.

Geostatistics

The Kf-1a parasequence in the Ivie Creek case-study area has been subdivided into three general facies: proximal delta front, medial delta front, and distal delta front. During the quarter a detailed block of outcrop from the south-facing Ivie Creek photomosaic was selected for statistical analysis. The net footage and relative percentage of each sedimentary structure, biologic structure, average megascopic grain size, and sandstone/shale ratio were calculated for the three facies (Fig. 7). Horizontal bedding is the most common sedimentary structure in all three facies (Fig. 7a). Ripple cross-laminated beds are the second most common sedimentary structure in the distal delta-front and medial delta-front facies while trough cross-stratified beds are second in proximal delta-front facies. As expected, the proximal delta-front facies contains the coarsest material and highest net portion of sandstone while the distal delta-front facies contains the finest material and lowest portion of sandstone (Figs. 7b and 7c).

Photomosaic Scaling

Dimensional data from the Kf-1a parasequence in the Ivie Creek case-study area, for which detailed reservoir models will be developed, need to be determined at a high level of precision. To achieve this, clinoform boundaries in the Kf-1a parasequence identified on photomosaics were digitized during the quarter. Field survey data collected in the previous quarter were reduced to x-y-z coordinates to be used in making the three-dimensional geologic model. All scaling of the photomosaics was completed and elevation profiles were created using the Kf-1/Kf-2 boundary as a datum, and the data input into a spreadsheet. General facies categories were assigned to units on the photomosaic panels based on geometry, sedimentary structures, and apparent shale content. Utilizing tie points on the panels that were identified in the field, the elevation profile picks were positioned on the 7.5 minute topographic maps and will form the base for construction of the three-dimensional model of the reservoir architecture.

Stochastic Modeling and Fluid-Flow Simulation

Although no fluid-flow simulations were carried out this quarter, the three-dimensional version of the homogenization routine was completed, work was initiated on including this routine in the TETRAD3-D black oil simulator, and the first phase of developing a stochastic approach for creating synthetic groups of clinoforms was completed. These numerical routines will be used in subsequent quarters to complete the fluid-flow simulation tasks.

Three-Dimensional Homogenization Codes

A group of three-dimensional homogenization codes were written to determine effective permeabilities for porous media problems. The codes include four different averaging methods; (1) homogenization, (2) arithmetic averaging, (3) geometric averaging, and (4) harmonic averaging. The homogenization method implemented in the code was originally developed by Bourgeat.[7] The other averaging techniques are implemented to provide a basis for comparing effective permeabilities determined using traditional methods to the homogenization results. The code package includes a finite element formulation of a black oil simulator that solves the fluid-flow equations on a rectangular grid. Because the homogenization method is flow based, it provides an improved methodology for averaging and upscaling the fine-scale permeability information. A comprehensive report entitled *Documentation and Installation Guide for HomCode: A Code for Scaling up Permeabilities Using Homogenization* was prepared and will be released as a UGS contract report in the near future.

Creating Synthetic Clinoforms

Data collected during 1995 suggests that sufficient information has been obtained to create synthetic patterns of permeability within clinoform shapes. A stochastic code has been developed and is being tested for generating packages of stacked clinoform-like objects that resemble the features mapped in the Kf-1a parasequence. Originally developed using Mathematica, the code was reformulated in FORTRAN to ensure portability.

The code uses geometrical parameters (such as slope, total height, and total length) from

photomosaic measurements to create a series of two-dimensional clinoform-like objects. Figure 8 shows two typical results. Note the degree of variability in thickness, character of pinchouts, and general clinoform style within each model domain. Additional work is required to more completely integrate the geological interpretations with the mathematical routines. The goal is to use this code to generate synthetic clinoform structures then distribute permeability values within each object using rules derived from the permeability transects and detailed geological mapping. The resulting permeability structure will form the basis for a series of fluid-flow simulations that demonstrate the impact of the clinoform features on oil production.

Technology Transfer

A project overview was presented on July 14, 1995 to the UGS Board of Directors, Emery County commissioners and planning officials, industry representatives, and the local press. The project objectives and description, accomplishments, and potential benefits were discussed. The presentation was followed by a field trip to the Ivie Creek case-study area. On August 17, 1995, information on the coalbed methane potential of the Ferron Sandstone (currently the most active gas play in Utah) was presented at a public meeting sponsored by the U.S. Bureau of Land Management in Price, Utah. The Ferron project was reviewed and derivative resource maps were displayed and discussed. Three television networks carried coverage of the meeting; media coverage generated numerous inquiries.

Project materials were displayed at the UGS booth during the American Association of Petroleum Geologists (AAPG) Rocky Mountain Section meeting held in Reno, Nevada, July 16-19, 1995. Project team members presented seven papers describing Ferron sequence stratigraphy, project methods, and Ferron reservoir models.[8-14] The UGS also released the July 1995 issue of *Petroleum News* featuring the Ferron project. Three abstracts (Ferron statistical analysis, reservoir modeling, and coalbed methane potential) were submitted for presentation at the 1996 AAPG national convention in San Diego, California.

References

1. J. C. Van Wagoner, R. M. Mitchum, K. M. Campion, and V. D. Rahmanian, Siliciclastic Sequences, Stratigraphy in Well Logs, Cores and Outcrops: *Amer. Assoc. Petr. Geol., Methods in Exploration,* (7), 55 (1990).

2. C. H. Sondergeld and C. S. Rai, *Geophysical evaluation module operator's manual,* Amoco Research Report T88-E-0033: (1988).

3. C. H. Sondergeld and C. S. Rai, A New Concept in Quantitative Core Characterization, *The Leading Edge*: 774-779 (July 1993).

4. C. H. Sondergeld and C. S. Rai, A New Exploration Tool: Quantitative Core Characterization, *PAGEOPH*, 141 (2/3/4): 249-268 (1993).

5. E. Schreiber, O. L. Anderson, and N. Soga, *Elastic Constants and Their Measurement,*

McGraw-Hill, New York: 196 pp. (1973).

6. P. R. Griffiths and J. A. de Haseth, *Fourier Transform Infrared Spectrometry*, John Wiley, New York: (1986).

7. A. Bourgeat, Homogenization Method Applied to the Behaviour of a Naturally Fissured Reservoir, *Mathematical Methods in Energy Research* (K. I. Gross, Ed.), Soc. Indust. & Appl. Math.: 181-193, 1984.

8. R. D. Adams, The Cretaceous Ferron Sandstone of East-Central Utah: A Tale of Three Different Morphologies for Deltaic Parasequences, *Am. Assoc. of Petr. Geol. Bull.* 79(6): 914 (June 1995).

9. R. D. Adams, S. H. Snelgrove, and C. Forster, A Methodology for Obtaining Detailed Geologic Descriptions to Constrain 3-D Reservoir Fluid-Flow Simulation Models in Delta-Front Lithofacies, *Am. Assoc. of Petr. Geol. Bull.* 79(6): 914 (June 1995).

10. P. B. Anderson and T. A. Ryer, Proposed Revisions to Parasequence-Set Nomenclature of the Upper Cretaceous Ferron Sandstone Member of the Mancos Shale, *Am. Assoc. of Petr. Geol. Bull.* 79(6): 914-915 (June 1995).

11. T. C. Chidsey, Jr., Geological and Petrophysical Characterization of the Ferron Sandstone in Utah, For 3-D Simulation of a Fluvial-Deltaic Reservoir, *Am. Assoc. of Petr. Geol. Bull.* 79(6): 916 (June 1995).

12. J. A. Dewey, Jr., T. H. Morris, and T. A. Ryer, Constraining Reservoir Models of Fluvial- vs. Wave-Dominated Delta-Front Sandstones through High Resolution and High Density Sequence Stratigraphic Analysis, Ferron Sandstone, Utah, *Am. Assoc. of Petr. Geol. Bull.* 79(6): 917 (June 1995).

13. T. A. Ryer and P. B. Anderson, Parasequence Sets, Parasequences, Facies Distributions, and Depositional History of the Upper Cretaceous Ferron Deltaic Clastic Wedge, Utah, *Am. Assoc. of Petr. Geol. Bull.* 79(6): 924 (June 1995).

14. T. A. Ryer, J. A. Dewey, Jr., and T. H. Morris, Distinguishing Allocyclic and Autocyclic Causes of Parasequence-Level Cyclicity--Lessons from Deltaic Strata of the Upper Cretaceous Ferron Sandstone, Central Utah, *Am. Assoc. of Petr. Geol. Bull.* 79(6): 924 (June 1995).

NEXT QUARTER PLANNED ACTIVITIES

Activities planned for the next quarter include:

1. Continue plotting locations of measured sections, paleocurrent sites, and gamma-ray and mini-permeameter transects on base maps. Complete production of columnar presentations of new measured-section data and rose diagrams of paleocurrents using computer software designed for the display of stratigraphic data. Post paleocurrent rose diagrams on the digital base maps.

2. Complete graphical log displays of gamma-ray measurements taken from outcrops in the Ivie Creek case-study area.

3. Complete cataloging and printing of digitized ground-based and aerial photographs, and construction of photomosaics for regional stratigraphic and case-study analysis.

4. Complete regional outcrop mapping and interpretation in the field.

5. Describe core from the new core hole in the Ivie Creek case-study area, enter the data into the database, and draft columnar log.

6. Document 1995 mini-permeameter results in spreadsheet and graphic format.

7. Begin petrophysical analysis of samples from the 1995 core-plugging program.

8. Create kriged surfaces from elevation data of the photomosaics. Complete digitizing versions of geologic trace maps with a grid. Edit the clinoform digitized data to form closed polygons and incorporate permeability data. Produce gridded cross sections as a basis for constructing digital fence diagrams. Simulate two-dimensional cross sections mapped by the project field team.

9. Continue quantifying sedimentary and petrophysical data to develop statistical models.

10. Publish as a UGS contract report, the computer codes describing the method in intuitive terms and how to use the codes. Modify TETRAD, the modeling program provided by Mobil, to test the homogenization methods in real oil industry simulators. The modifications require the inclusion of full tensor permeabilities.

11. Begin production of cross sections and lithofacies maps for the case-study areas.

12. Complete thin section work.

13. Conduct the following technology transfer activities: (a) prepare and present a paper on the Ferron project to the geology department at Idaho State University, Pocatello, Idaho, (b) write at least two abstracts on the project (regional sequence stratigraphy and Ivie Creek case-study geology) and submit for presentation at the 1996 AAPG Rocky Mountain Section meeting in Billings, Montana, (c) prepare the January 1996 issue of the UGS *Petroleum News*.

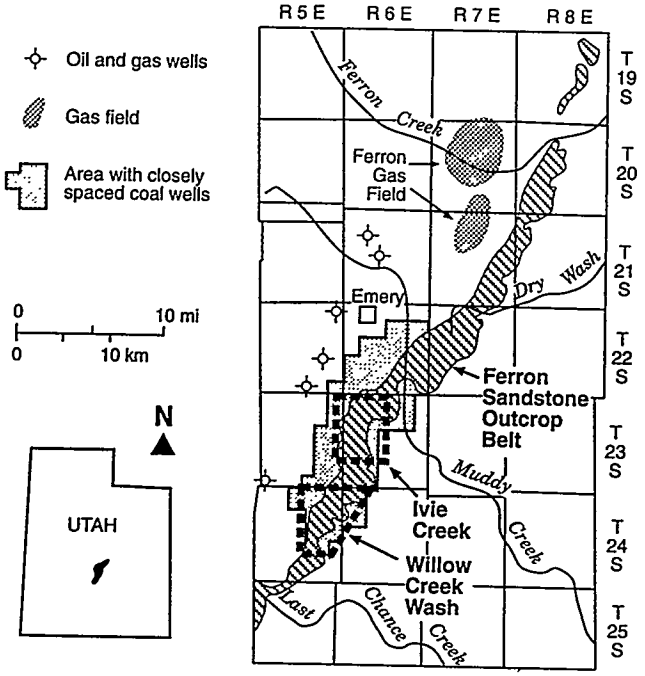
Oil and gas wells
Gas field
Area with closely spaced coal wells
0
10 mi
0
10 km
N
UTAH
R5E
R6E
R7E
R8E
T 19 S
T 20 S
T 21 S
T 22 S
T 23 S
T 24 S
T 25 S
Ferron Creek
Ferron Gas Field
Dry Wash
Emery
Ferron Sandstone Outcrop Belt
Muddy
Ivie Creek
Willow Creek Wash
Last Chance Creek
Creek

FIG. 1

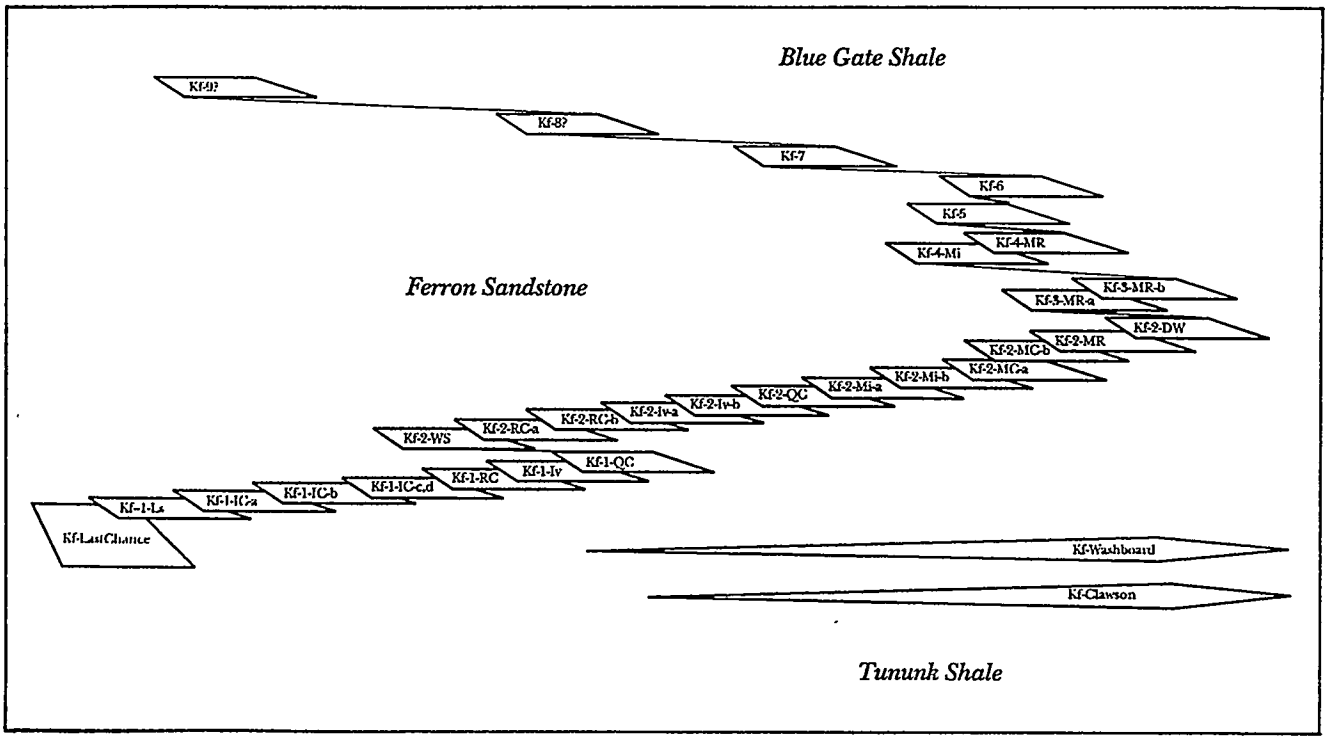
Blue Gate Shale
Kf-9?
Kf-8?
Kf-7
Kf-6
Kf-5
Kf-4-MR
Kf-4-Mi
Ferron Sandstone
Kf-3-MR-b
Kf-3-MR-a
Kf-2-DW
Kf-2-MR
Kf-2-MC-b
Kf-2-MC-a
Kf-2-Mi-b
Kf-2-Mi-a
Kf-2-QC
Kf-2-Iv-b
Kf-2-Iv-a
Kf-2-RC-b
Kf-2-RC-a
Kf-2-WS
Kf-1-QC
Kf-1-Iv
Kf-1-RC
Kf-1-IC-c,d
Kf-1-IC-b
Kf-1-IC-a
Kf-1-Ls
Kf-LastChance
Kf-Washboard
Kf-Clawson
Tununk Shale

FIG. 2

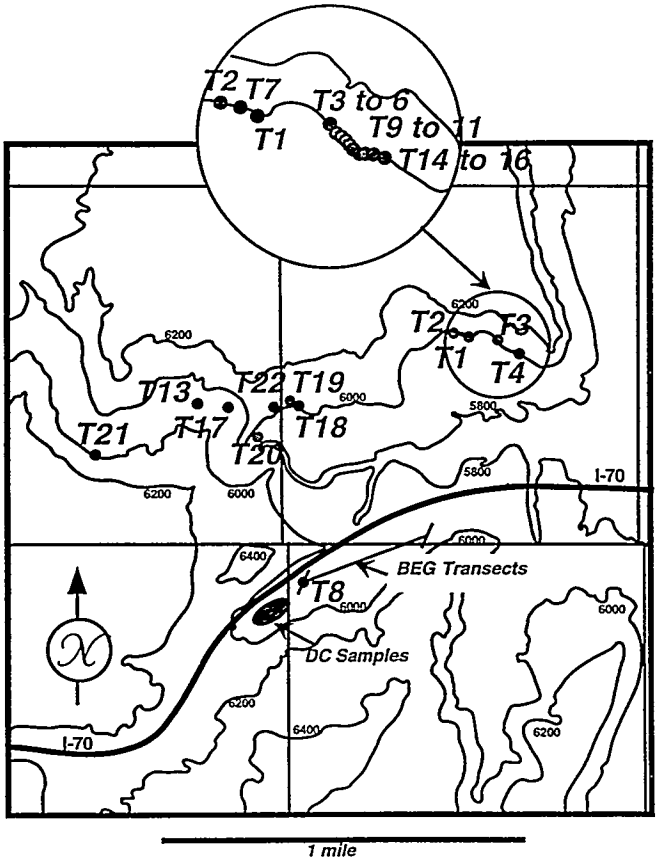
T2 T7
T3 to 6
T1
T9 to 11
T14 to 16
T2
T3
T1
T4
T13
T22
T19
T21
T17
T18
T20
6200
6000
5800
6400
I-70
BEG Transects
T8
DC Samples
N
1 mile

FIG. 3

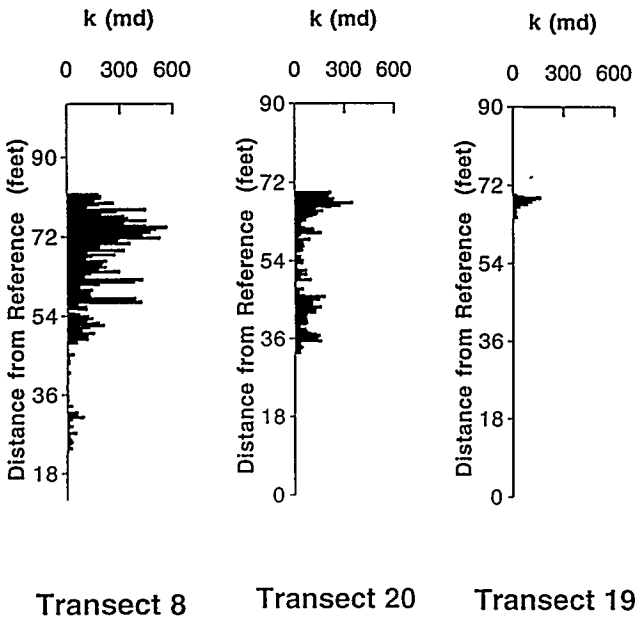
k (md)
0 300 600
90
72
54
36
18
Distance from Reference (feet)
k (md)
0 300 600
90
72
54
36
18
0
Distance from Reference (feet)
k (md)
0 300 600
90
72
54
36
18
0
Distance from Reference (feet)
Transect 8
Transect 20
Transect 19

FIG. 4

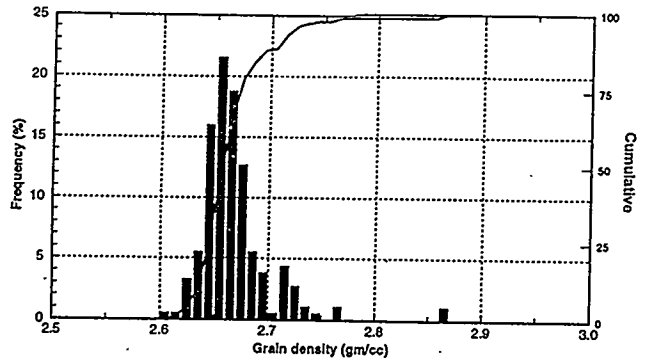
Frequency (%)
Cumulative
Grain density (gm/cc)
25
20
15
10
5
0
100
75
50
25
0
2.5
2.6
2.7
2.8
2.9
3.0

(A)

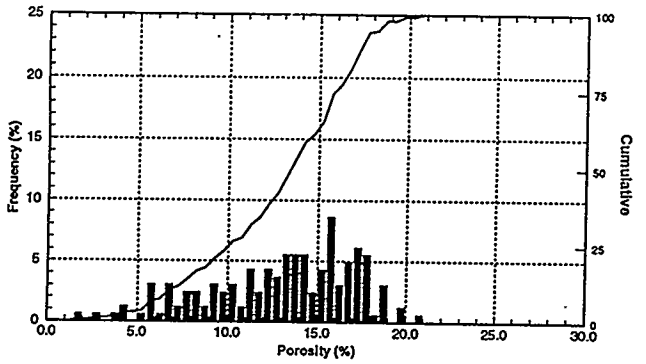
Frequency (%)
Cumulative
Porosity (%)
25
20
15
10
5
0
100
75
50
25
0
0.0
5.0
10.0
15.0
20.0
25.0
30.0

(B)

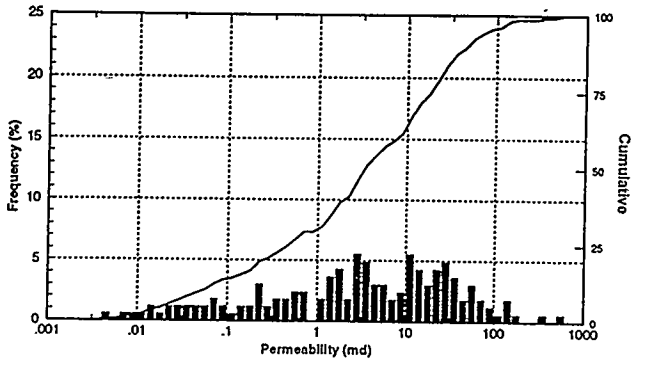
Frequency (%)
Cumulative
Permeability (md)
25
20
15
10
5
0
100
75
50
25
0
.001
.01
.1
1
10
100
1000

(C)

FIG. 5

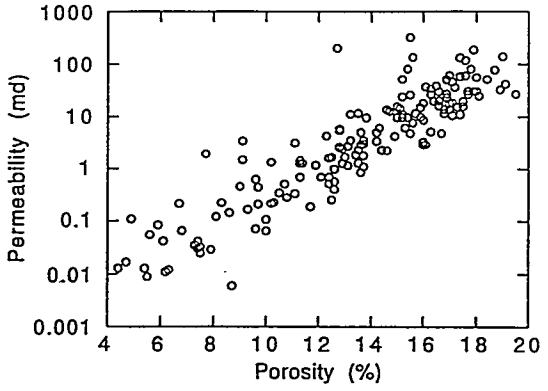
1000
100
10
1
0.1
0.01
0.001
Permeability (md)
4
6
8
10
12
14
16
18
20
Porosity (%)

(A)

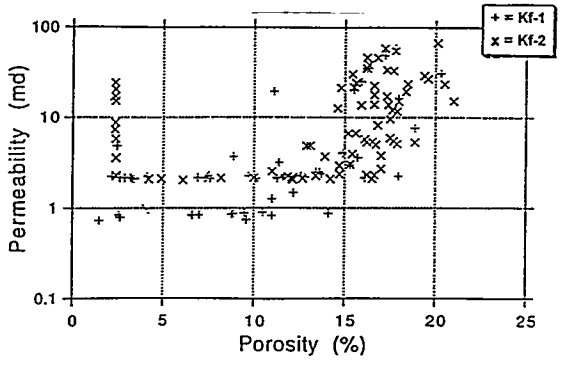
+ = Kf-1
x = Kf-2
100
10
1
0.1
Permeability (md)
0
5
10
15
20
25
Porosity (%)

(B)

FIG. 6

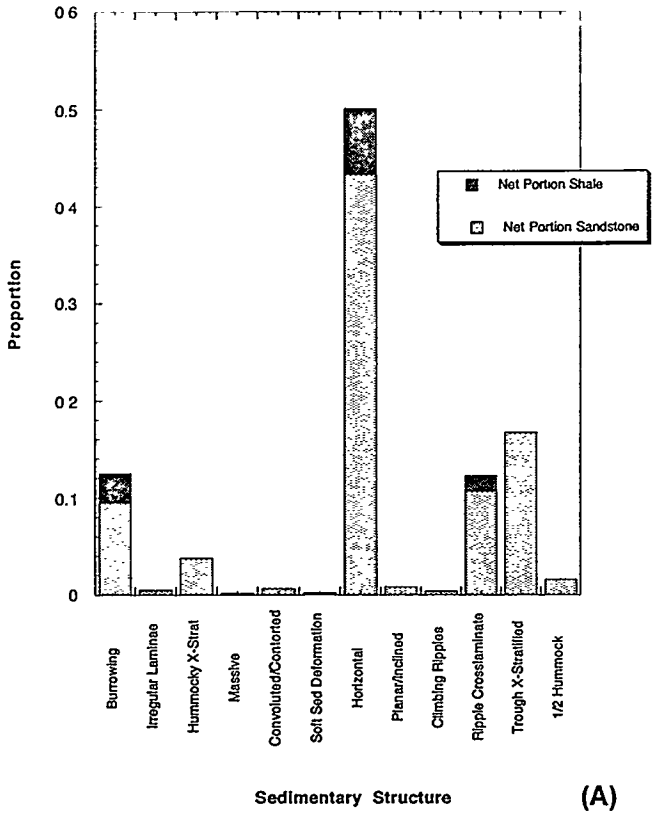
0.6
0.5
0.4
0.3
0.2
0.1
0
Proportion
Net Portion Shale
Net Portion Sandstone
Burrowing
Irregular Laminae
Hummocky X-Strat
Massive
Convoluted/Contorted
Soft Sed Deformation
Horizontal
Planar/Inclined
Climbing Ripples
Ripple Crosslaminate
Trough X-Stratified
1/2 Hummock
Sedimentary Structure
(A)

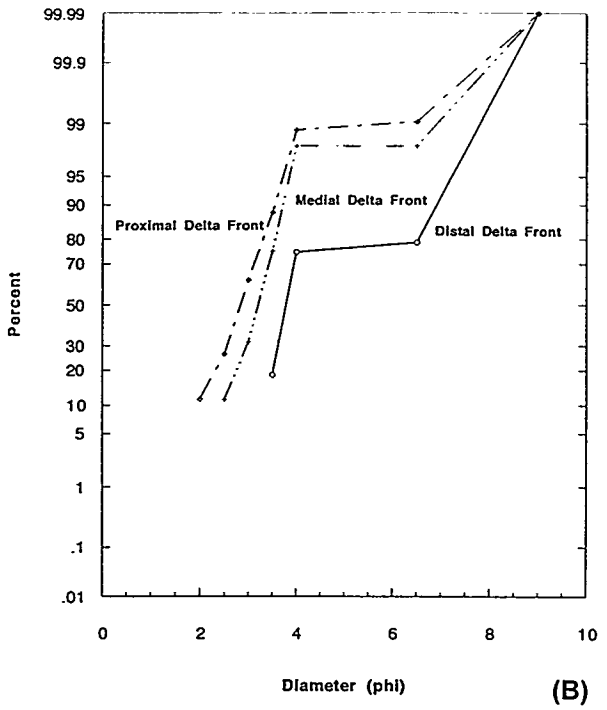
99.99
99.9
99
95
90
80
70
50
30
20
10
5
1
.1
.01
Percent
Proximal Delta Front
Medial Delta Front
Distal Delta Front
0
2
4
6
8
10
Diameter (phi)
(B)

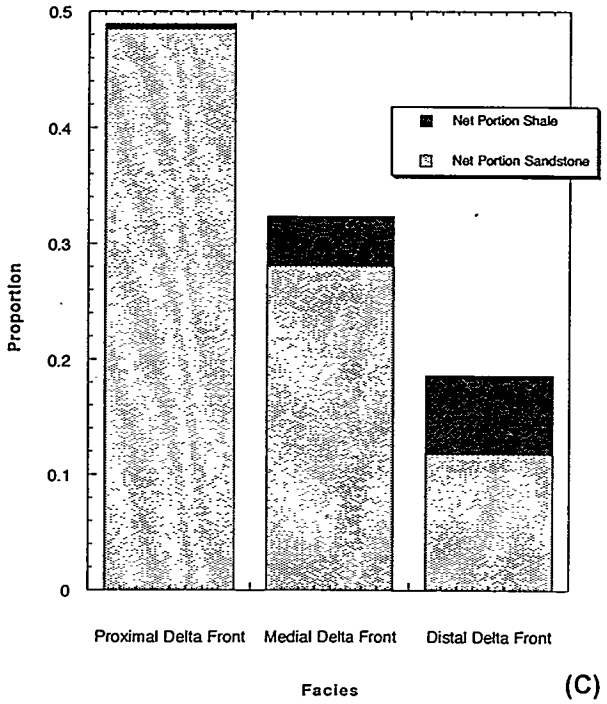
0.5
0.4
0.3
0.2
0.1
0
Proportion
Net Portion Shale
Net Portion Sandstone
Proximal Delta Front
Medial Delta Front
Distal Delta Front
Facies
(C)

FIG. 7

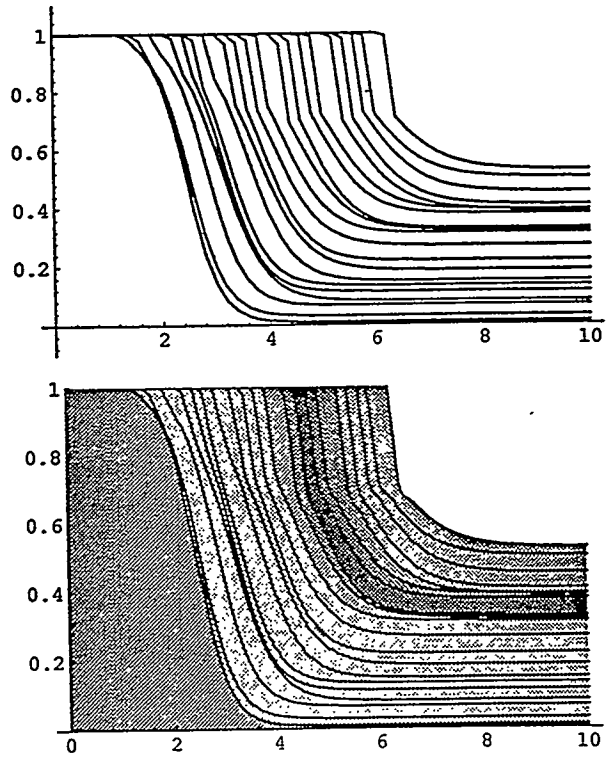

FIG. 8

FIGURE CAPTIONS

Fig 1. Location map of the Ferron Sandstone study area (outcrop belt cross-hatched) showing detailed case-study sites (outlined by heavy dashed lines).

Fig 2. Diagram showing relative positions of Ferron parasequences and parasequence sets. The diagram has no scale. Landward is to the left, seaward to the right. The vertical axis is probably better equated to time than to rock section. Note that parasequence sets Kf-5, Kf-6, and Kf-7 are presently not divided into parasequences. Kf-8? and Kf-9? are shoreline sandstone units that have been recognized but not yet formally incorporated into the scheme.

Fig. 3. Map showing permeability sampling transect locations at the Ivie Creek case-study area. BEG transects refers to the location of permeability transects conducted by the Texas Bureau of Economic Geology.

Fig. 4. Permeability as a function of vertical position within the Kf-2 parasequence set at transects T8, T20, and T19.

Fig. 5. Histograms of: (A) grain densities, (B) porosity, and (C) permeability, along with their respective cumulative frequency distributions (sloped line) for 182 Ferron core plugs collected during the 1994 field season and processed through Amoco Production Research's Geoscience Evaluation Module (GEM).

Fig. 6. Relationship between permeability and porosity, based on core-plug measurements of the Ferron Sandstone: (A) overall permeability and porosity from GEM processing. (B) permeability and porosity comparing the Kf-1 and Kf-2 sandstones processed at the University of Utah (where permeability was measured using a mini-permeameter). Note the inaccuracy of the mini-permeameter for <5 md, and the strong linear relationship identified by the GEM measurements.

Fig. 7. Statistical analyses of a detailed block of the Kf-1a parasequence in the Ivie Creek case-study area: (A) net sandstone versus sedimentary structure, (B) cumulative frequency grain size (based on average megascopic observations) for each facies, and (C) net sandstone versus facies.

Fig. 8. Sample of two clinoform-like objects created using a stochastic approach (in arbitrary length units). Slightly different rules were used to generate the two different versions. Note that the top of each clinoform meets the upper boundary of the domain at a relatively shallow angle in the upper version.